Raman characterization studies of synthetic and natural $MgAl_2O_4$ crystals

Lewis M. Fraas, James E. Moore, and José B. Salzberg

Institute de Física "Gleb Wataghin," Universidade Estadual de Campinas, Campinas, São Paulo, Brasil

(Received 31 July 1972)

Raman studies are reported for one natural and four synthetic $MgAl_2O_4$ spinel crystals and symmetry assignments for the phonon modes of the spinel crystal structure are given. Deviations in the Raman selection rules are observed for the synthetic spinel crystals in the form of additional modes over and above those theoretically predicted. Also, detailed studies of one of the synthetic crystals show a probable disordering in the Mg–Al sites. Raman linewidths and violations of selection rules, as reported here, can aid in the characterization and quality control of synthetically grown crystals.

INTRODUCTION

Raman studies of magnon modes in the spinel crystal, $CdCr_2Se_4$, have been reported by Harbeke and Steigmeier[1] and Koningstein *et al.*[2] have reported electronic Raman modes from Co^{3+} in Co_2GeO_4 spinel. However, despite these extended mode studies, no detailed Raman polarization studies for the phonon modes of a spinel crystal have been undertaken. It would seem that such work would be quite useful for future electronic and magnon mode studies.

The results of Raman polarization studies for the phonon modes of $MgAl_2O_4$ are reported here and some frequency assignments are made. These results complement phonon mode studies in $MgAl_2O_4$ via host lattice infrared absorption,[3] impurity absorption,[4] and fluorescence,[5] as well as some Raman phonon studies of microcrystalline spinel group minerals.[6]

In the early phase of this work, it was found that the polarizability tensors measured for the first synthetic $MgAl_2O_4$ crystal were in disagreement with those predicted by a normal mode analysis by Lutz.[7] In order to understand these Raman selection rule violations, studies of additional crystals were undertaken. In all, results for five $MgAl_2O_4$ spinel crystals are reported here. It is found that synthetic crystals are, by in large, of poorer quality than natural crystals. The Raman selection rules are found to hold for our natural crystal despite probable resonance with impurities and a deviation from stoichiometry. The synthetic crystals show disordering effects. These effects are interesting in terms of quality control in crystal growth especially since $MgAl_2O_4$ spinel is becoming an important substrate material for silicon epitaxy MOS integrated circuits.[8]

EXPERIMENT

The properties of the five crystals studied are summarized in Table I. Of the five, four were synthetic and one was natural. The four synthetic crystals were obtained through the cooperation of Linde Division, Union Carbide Corporation. The first synthetic crystal obtained (No. 1 in Table I) was a Czochralski grown colorless crystal,[9] considered by the manufacturer to be nearly stoichiometric and nominally pure. Of the remaining synthetic crystals, one was red (No. 3) with an appreciable Cr^{3+} impurity content; another was a blue-green crystal (No. 4) with an appreciable V^{3+} content, and the last was a small nominally pure transparent crystal (No. 5). The natural crystal was a small red-orange crystal (No. 2) obtained in Brasil. This crystal had both V^{3+} and Cr^{3+} impurities.

All the crystals were carefully oriented by x-ray Laue photographs, then cut and polished such that Raman polarization studies could be made on the (100) crystallographic orientation.

The first synthetic crystal was cut and polished

TABLE I. Crystal characteristics.

No.	Color	Impurities	Growth	Comments
1	clear	nominally pure	synthetic	Reportedly stoichiometric
2	orange	Cr, V	natural	
3	red	Cr	synthetic	
4	blue	V	synthetic	Laue patterns show crystal strains
5	clear	nominally pure	synthetic	Laue patterns show crystal strains

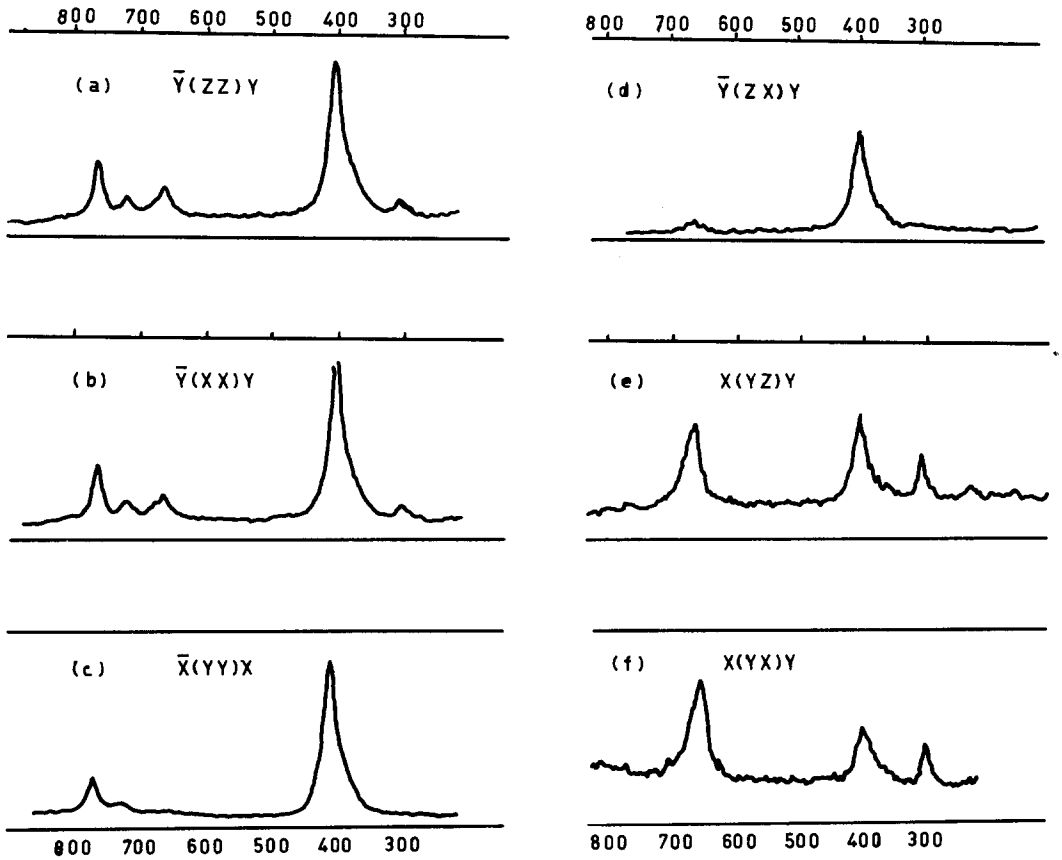

FIG. 1. Raman polarization spectra of No. 1 using argon laser excitation. (a) $\bar{Y}(ZZ)Y$, 5145 Å; (b) $\bar{Y}(XX)Y$, 5145 Å; (c) $\bar{X}(YY)X$, 5145 Å; (d) $\bar{Y}(ZX)Y$, 5145 Å; (e) $X(YZ)Y$, 5145 Å, high gain; (f) $X(YX)Y$, 4880 Å, high gain.

in such a way that the (111) set of polarization components could be studied as well. The natural faces (111) of No. 2 allowed the (111) set of polarization components for this crystal to be compared with the pure stoichiometric crystal No. 1.

The Raman spectra were taken with an Ar ion laser and a Spex double monochromator. The method used is conventional and is explained in Ref. 10. The fluorescence spectra of Cr^{3+} and V^{3+} were also taken with the same experimental setup. All the Raman spectra reported here were taken with 8 cm^{-1} spectrometer resolution.

RESULTS

Raman spectra of No. 1 were first taken in the x, y, z axis system. These axes are defined as follows:

$$x=(111), \quad y=(1\bar{1}0), \quad \text{and} \quad z=(\bar{1}\bar{1}2).$$

The spectra for the complete Raman polarizability tensor in this reference frame are shown in Fig. 1. In these spectra, five reasonably strong lines are observed.

Group theory predicts for the normal spinel structure $1A_{1g}$, $1E_g$, and $3F_{2g}$ modes.[7] Furthermore, the A_{1g} modes will always be diagonal regardless of the crystal

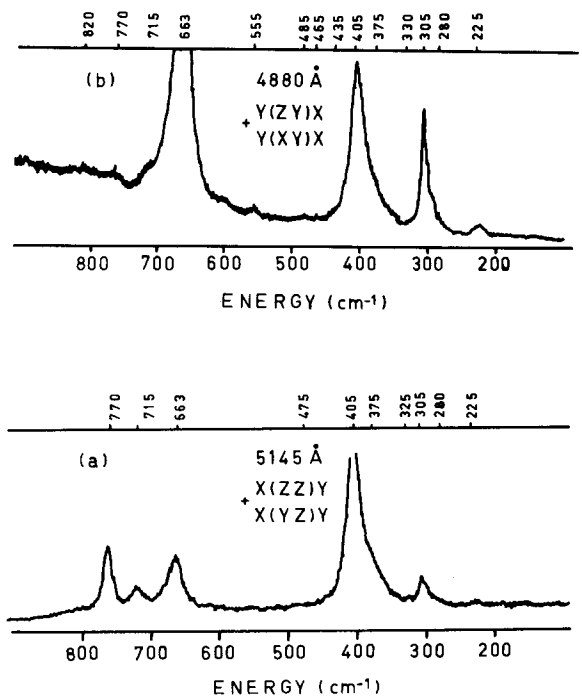

FIG. 2. High signal Raman spectra of No. 1.

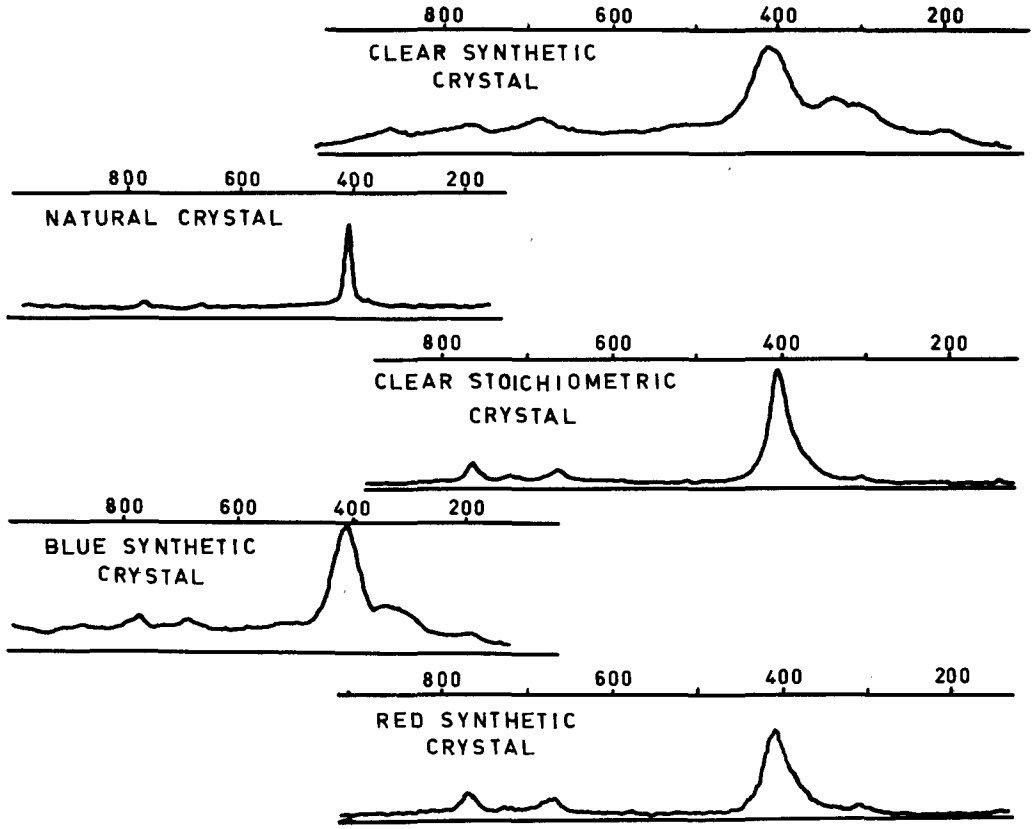

FIG. 3. Unpolarized Raman spectra of all five spinel crystals. Numbering spectra from top to bottom, the first and fourth spectra of Nos. 4 and 5, respectively, manifest the broadest features and lowest quality. Similarly, spectra 3 and 5 of Nos. 1 and 3, respectively, show these crystals to be of intermediate quality. Crystal No. 2, spectra 2, is of the highest quality.

orientation. This allows identification of A_{1g} modes immediately. In the present spectra, the modes identified as the A_{1g} correspond to the two modes with the greatest frequency shift from the laser line as shown in Fig. 1. In addition to this contradiction, the polarization information for the other three lines is also in contradiction with theory.

These contradictions of theoretical predictions led us to look for extra modes. Ten extra modes were found, as can be seen in the high signal to noise spectra shown in Fig. 2. These modes shift with laser frequency when spectra are taken with the 5145- and 4880-Å argon laser lines; thus, all are Raman modes.

In order to determine the reason for the selection rule violation observed in the first crystal, unpolarized, polarized, and depolarized Raman spectra were taken for all five crystals. These spectra are taken in the x', y', z' reference frame ($x'=100$, $y'=010$, and $z'=001$) and are shown in Figs. 3, 4, and 5. All these spectra were taken with 4579-Å Ar laser excitation in order to avoid V^{3+} fluorescence interference (see Fig. 8). It is clear from the linewidths of the Raman lines in these spectra that the natural crystal is of the highest quality; the synthetic crystals, Nos. 1 and 3, are of lower quality, while the synthetic crystals, Nos. 4 and 5, are of lowest quality. There are frequency shifts from crystal to crystal (evident in Fig. 3) and polarizability changes from crystal to crystal (Figs. 4 and 5).

Figure 6 shows Raman data, polarized and depolarized, taken on the natural crystal by back scattering from the (111) face. The experimental conditions were otherwise similar to those for Figs. 3–5. The spectra of Fig. 6 combined with those of Figs. 4 and 5 allow identification of the mode at 405 cm^{-1} as E_g, the mode at 663 cm^{-1} as F_{2g}, and the mode at 770 cm^{-1} as A_{1g}.

A further measure of crystal quality was made by taking the Cr^{3+} fluorescence spectra of each of the five crystals. These spectra are shown in Fig. 7. As was the case for the Raman spectra, the crystal qualities can be ranked in the following order: 2, 1, 3, 4, 5.

DISCUSSION

In this section the interesting features of the spectra of Figs. 1–8 are reviewed.

Problems with the Raman Polarizability Tensors

The spinel unit cell is shown in Fig. 9. The normal

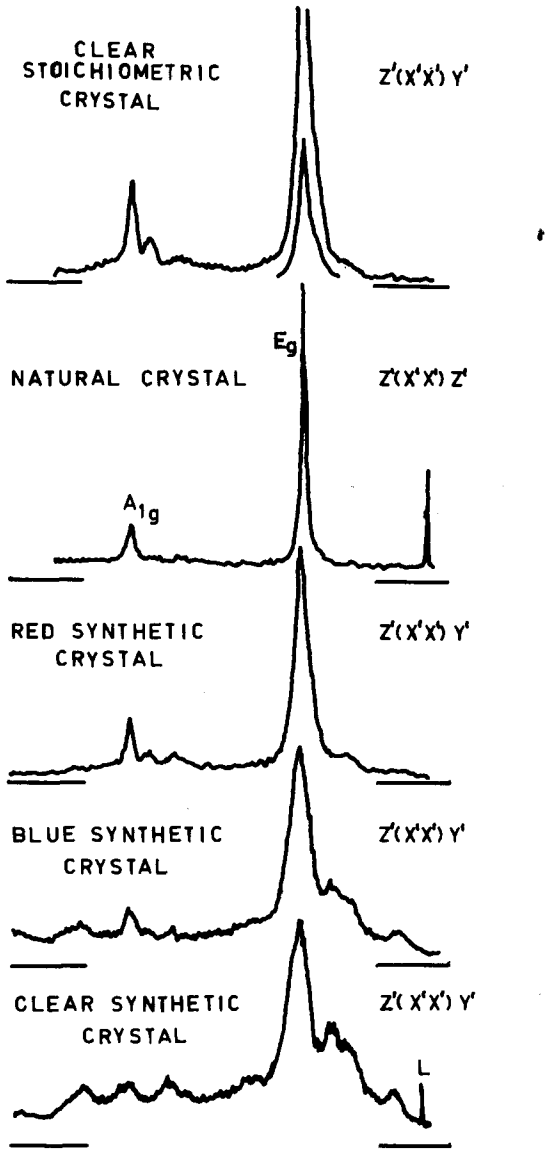

FIG. 4. Polarized Raman spectra for all five crystals. The E_g and A_{1g} modes are labeled for No. 2.

unit cell belongs to the cubic space group O_h^7 ($Fd3m$) with eight formula units per cell. The structure contains two kinds of metal ion sites. In the normal spinel, the Mg site has tetrahedral coordination with full T_d symmetry. The Al (or Cr) site has a sixfold distorted octahedral coordination. This site belongs to the D_{3d} point group. The trigonal axis of the D_{3d} group is coincident with the (111) axis of the crystal and has a center of inversion. The oxygen sites are C_{3v}. The irreducible representation for the optical modes of the crystal are:

$$1A_{1g}+2A_{2u}+1E_g+2E_u+1F_{1g}+4F_{1u}+3F_{2g}+2F_{2u}. \quad (1)$$

Of these, there are five Raman active modes: $1A_{1g}+1E_g+3F_{2g}$.

The Raman tensors in the crystallographic frame of reference are as follows:

$$A_{1g}: \; a\begin{bmatrix}1&0&0\\0&1&0\\0&0&1\end{bmatrix},$$

$$E_g: \; b\begin{bmatrix}1&0&0\\0&1&0\\0&0&-2\end{bmatrix}, \quad b\sqrt{3}\begin{bmatrix}1&0&0\\0&-1&0\\0&0&0\end{bmatrix},$$

$$F_{2g}: \; c\begin{bmatrix}0&1&0\\1&0&0\\0&0&0\end{bmatrix}, \quad c\begin{bmatrix}0&0&1\\0&0&0\\1&0&0\end{bmatrix}, \quad c\begin{bmatrix}0&0&0\\0&0&1\\0&1&0\end{bmatrix}.$$

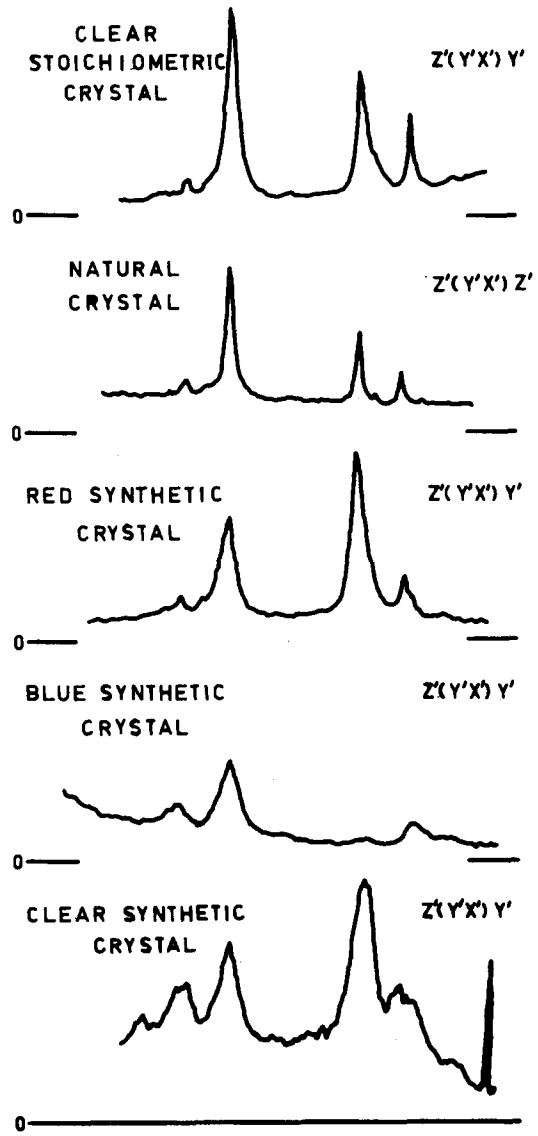

FIG. 5. Depolarized Raman spectra for all five crystals.

The transformation tensor to the laboratory frame is:

$$S^{-1}: \begin{bmatrix} 1/\sqrt{3} & 1/\sqrt{2} & 1/\sqrt{6} \\ 1/\sqrt{3} & -1/\sqrt{2} & 1/\sqrt{6} \\ 1/\sqrt{3} & 0 & -2/\sqrt{6} \end{bmatrix},$$

and the transformed polarizability tensors are then given by

$$a' = SaS^{-1}.$$

The final ij intensity components are calculated by summing the squares of the ij elements of the tensors for the phonons of each symmetry class. For example,

$$a_{xy}'^2(E_g) = a_{xy}'^2(E_g^a) + a_{xy}'^2(E_g^b).$$

The results of these calculations are shown in Table II.

If, for No. 1, the five modes in Fig. 1 are numbered 1–5 in order of increasing energy shift, then modes 4 and 5 are seen to have A_{1g} symmetry. Modes 1 and 3 behave similarly for Ar laser excitation and mode 2 is unique.

The measured polarizabilities for modes 2 and 3 of No. 1 are shown in Table II. The striking feature in these data is the occurrence of near zeros for xy and yz in mode 2 and again a near zero in yy for mode 3. The y direction is the $(1\bar{1}0)$ direction. There is no resemblance for either mode to the tensors for E_g and F_{2g}.

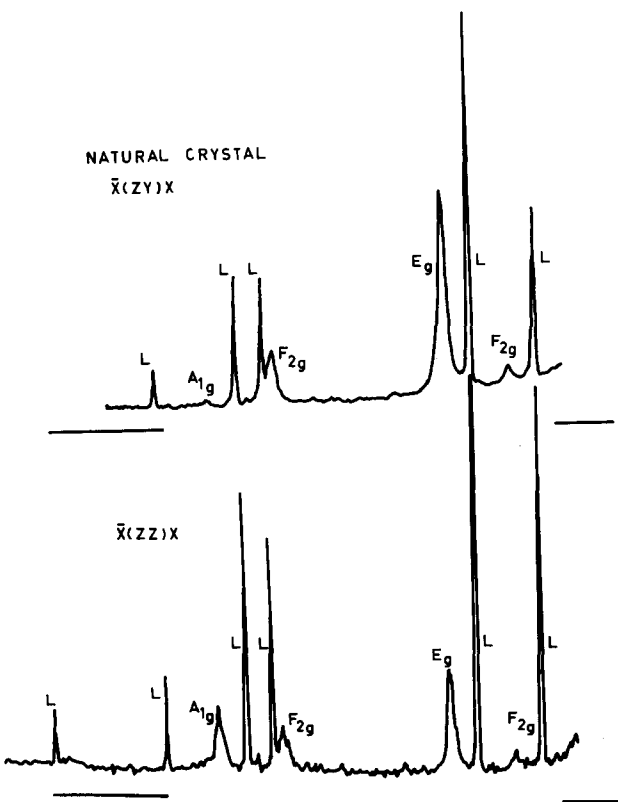

FIG. 6. Polarized and depolarized back-reflection Raman spectra for No. 2. The laser plasma lines are marked with L's. The Raman modes are labeled to indicate their respective symmetries.

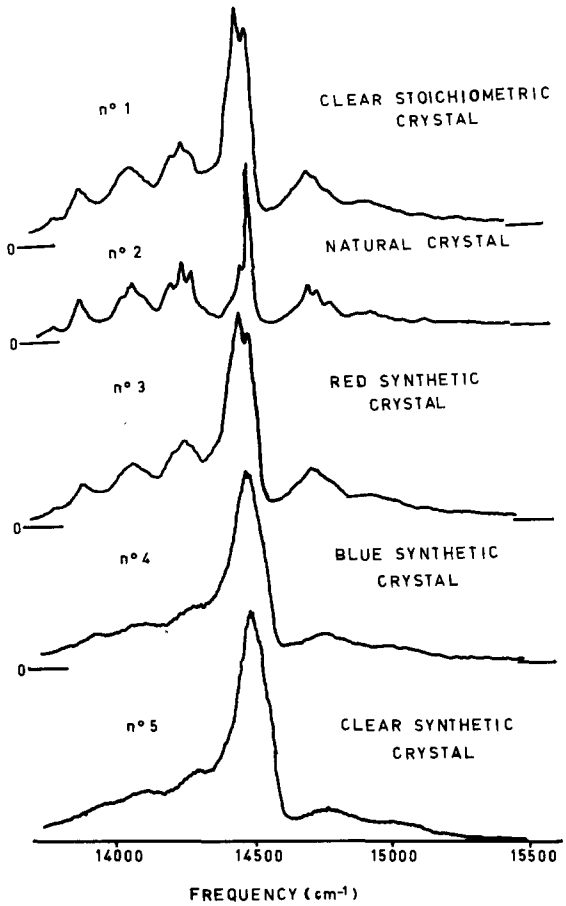

FIG. 7. Room temperature fluorescence spectra of the Cr^{3+} impurity in each of the five crystals. Note that the largest peak in the synthetic crystals is shifted to the pairing region.

In contrast to the selection rule violations for No. 1, the data of Figs. 4–6 can be used, in connection with the Raman tensors, to verify the validity of the Raman selection rules for the natural spinel crystal. First, note that the polarized spectra of Fig. 4, No. 2, compare well with the tensors of Eq. (2). Modes 1 and 3, F_{2g}'s, are not present. Modes 2 and 5, E_g and A_{1g}, respectively, are small in the spectra of Fig. 5. (The deviations from zero presumably result from a finite lens collection angle). Furthermore, in Fig. 6, if the ratio of the intensity of mode 2 to that of mode 3 in the polarized spectra is used with Table II to calculate b/c, then that value of b/c agrees within 3% with the b/c ratio calculated in a similar fashion from the depolarized spectra. It is therefore seen that the selection rules hold well for the natural crystal.

Number of Modes

Table III symmarizes the mode frequencies found in Fig. 2. Also listed are frequencies observed by other methods. Slack[3] has observed phonon modes in a single

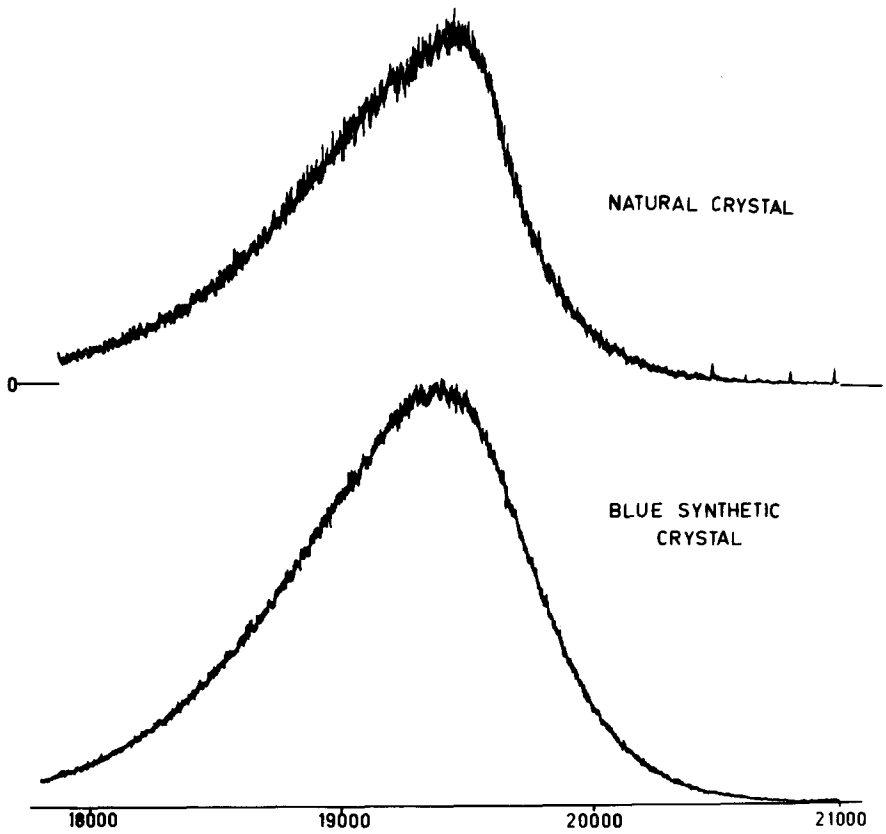

FIG. 8. The fluorescence spectra in the green-blue indicate the presence of V^{3+} impurities in Nos. 2 and 4.

crystal of $MgAl_2O_4$ by means of ir reflectivity. Slack, Ham, and Chrenko[4] have observed lattice phonon modes via optical absorption spectra of tetrahedral Fe^{2+} in $MgAl_2O_4$. Wood *et al.*[5] have observed lattice phonon modes in the fluorescence spectra of Cr^{3+}-doped $MgAl_2O_4$. The Raman spectra of Fig. 2(b) in which 15 modes are observed is seen to give the most complete picture of the phonon spectrum of spinel to date.

Crystal Quality and Growth of Spurious Modes

From the spectra of the natural crystal, it is clear that the features at 305, 405, 663, and 770 cm^{-1} are intrinsic to the normal spinel structure. The other features listed in Table III are seen to be generally larger in intensity as the crystal quality deteriorates. Since the spinel structure is quite complex, possessing 42 degrees of freedom, it is not too suprising that it is quite susceptible to various imperfections in growth and that these imperfections produce additional Raman modes.

In extended mode studies of spinel crystals, it is important to note that these additional modes can occur. For example, Koningstein *et al.*[2] report two peak structures in Co_2GeO_4, the first at 229 cm^{-1}, just on the lower frequency side of the allowed E_g mode, and the second at 900 cm^{-1}, just on the upper frequency side of the allowed A_{1g} mode. They assign these modes

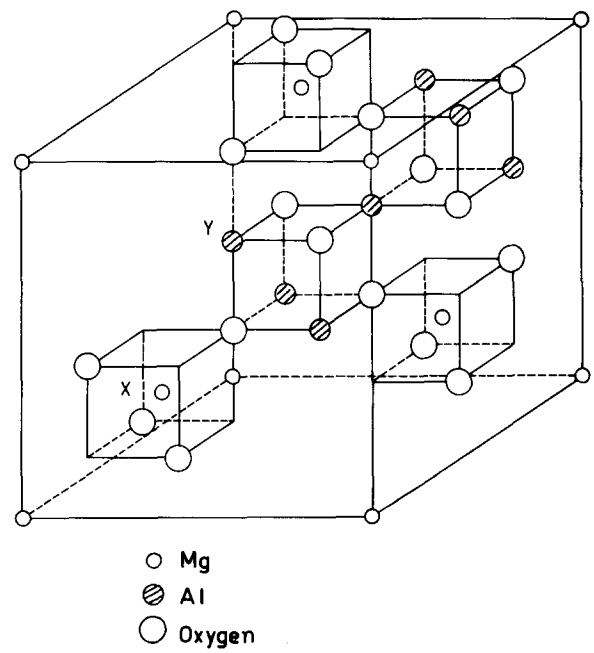

FIG. 9. The normal spinel unit cell is reproduced schematically as presented in Ref. 7. The letters X and Y indicate the Mg–Al pair switching found in an inverse spinel.

TABLE II. Relative polarizability intensities.

Mode	zz	xx	yy	xy	yz	xz
Calculated F_{2g} intensity	10	13.3	10	3.3	6.7	3.3
Observed mode 3 intensity	10	11	<2	11	19	8
Calculated E_g intensity	10	0	10	20	10	20
Observed mode 2 intensity	10	8.5	15	<2	<2	5

to electronic Raman scattering from Co^{3+}. It is noted that, in Figs. 3–5, our synthetic crystals, especially Nos. 4 and 5, show similar structure in the absence of Co^{3+}. Koningstein *et al.* have assigned these modes to E_g character, and as can be seen, our fifth crystal shows approximate E_g character for these same features. (See the features at 330 and 870 cm^{-1}.)

The Pairing Region of the Cr^{3+} Fluorescence Spectrum

The room temperature fluorescence spectra of Fig. 7 are in substantial agreement with the spectra reported by Wood *et al.*[5] The fluorescence spectra for the natural crystal are the clearest. Wood assigns the structure on the low-frequency side of the peak at 14 600 cm^{-1} largely due to phonons. However, the region on the low-energy side for small energy shifts between 0 and 200 cm^{-1} is assigned to Cr^{3+} pairing. He observes that there is some question as to whether this pairing arises through Cr^{3+}–Cr^{3+} pairs or Cr^{3+}–vacancy pairs. It should be noted that the anomalous pairing is strongest in the synthetic crystals.

TABLE III. Phonon frequency data.

Raman freq.	Raman intensity	Crystal ir[a]	Fe^{2+} ir[b]	Cr^{3+} fluor[c]
225 cm^{-1}	medium		220	218
280	weak			251
305	mode 1 strong	302		300
330	weak			
375	shoulder		365	
405	mode 2 strong			395
435	shoulder		450	447
463	weak	475		
485	weak		500	490
555	weak	530	550	
600	weak	580		
663	mode 3 strong			650
715	mode 4 strong	735		745
770	mode 5 strong		775	
825	weak			

[a] See Ref. 3.
[b] See Ref. 4.
[c] See Ref. 5.

INTERPRETATION

A priori, there are three possible explanations for the anomalies described in the previous section. The first is Cr^{3+} resonance. The second is nonstoichiometry. The third is complete or partial disorder in the Mg–Al positions.

Although we were able to observe Cr^{3+} resonance in No. 3 as is summarized in Table IV, this in itself does not explain the violation in selection rules for No. 1, modes 2 and 3. This follows because the Cr^{3+} content is higher in the natural crystal than in No. 1, yet the Raman selection rules are obeyed.

Nonstoichiometry does not seem to be the explanation since natural crystals are usually nonstoichiometric and No. 1 is reportedly reasonably stoichiometric. Thus the anomalies in the tensors for modes 2 and 3 of the stoichiometric crystal are again unexplained.[11] Therefore, the anomalies are probably attributed to disorder in the Mg–Al sites.

The observed Raman tensors for the modes 2 and 3

TABLE IV. Resonance data (No. 3). The ratio of the intensity of mode 2 to that of mode 5 is given as a function of laser excitation frequency.

Run	4579 Å	4880 Å	5145 Å
1	4.25	5.24	5.60
2	4.50	5.47	5.55 (190 mW)
3	4.70	5.17	5.50 (600 mW)
Averaged	4.50	5.29	5.55

of No. 1 have the following forms:

$$\text{Mode 2:} \begin{bmatrix} - & 0 & - \\ 0 & - & 0 \\ - & 0 & - \end{bmatrix},$$

$$\text{Mode 3:} \begin{bmatrix} - & - & - \\ - & 0 & - \\ - & - & - \end{bmatrix}.$$

The problem is to explain the obvious importance of the $(1\bar{1}0)$ axes.

If the Mg at site X in Fig. 9 is switched with the Al at site Y, the result is the start of an inverse spinel. There is evidence for this pairing anomaly in synthetic crystals of $MgAl_2O_4$ in earlier literature.[12,13] $MgFe_2O_4$, grown by nature, forms in the inverse structure. Other spinels are found with complete ranges from normal to inverse.[14] The pairing anomaly formed by switching Mg and Al ions lowers the symmetry of the oxygen site from C_{3v} to C_s. The highest symmetry element of this C_s site is a reflection plane with a normal along the $(1\bar{1}0)$ axis. This type of pair irregularity might explain as well the anomalously high fluorescence in the pairing region, for the synthetic crystals as observed in Fig. 7. Thus the Mg–Al disorder pairing explains qualitatively the spectral anomalies for No. 1. The near zeros are still, however, not quantitatively explained.

CONCLUSIONS

Because of the large number of ferrite spinels, the utility of the phonon frequency information obtained here is apparent. This paper also shows that the Raman effect can be of value in quality control for the growth of synthetic crystals. The fact that the resonant Raman effect can be seen from Cr^{3+} impurities is of possible interest as well.

ACKNOWLEDGMENTS

The authors are grateful to Professor S. P. S. Porto for furnishing us with the synthetic spinel crystals, and to Professor Marcelo Damy for providing the natural spinel crystal. The technical assistance of Mr. Marcelo Fossey is also gratefully acknowledged.

[1]E. F. Steigmeier and G. Harbeke, Phys. Kondens. Mater. **12,** 1 (1970).
[2]J. A. Koningstein, P.A. Grunberg, J. T. Hoff, and J. M. Preudhomme, J. Chem. Phys. **56,** 354 (1972).
[3]G. A. Slack, Phys. Rev. A **134,** 1268 (1964).
[4]G. A. Slack, F. A. Ham, and R. M. Chrenko, Phys. Rev. **152,** 376 (1966).
[5]D. L. Wood, G. F. Imbush, R. M. Macfarlane, P. Kesliuk, and D. M. Larkin, J. Chem. Phys. **48,** 5255 (1968).
[6]W. P. Griffith, J. Chem. Soc. A **1970,** 286 .
[7]H. D. Lutz, Z. Naturforsch. A **14,** 1417 (1969).
[8]J. E. A. Maurits and A. M. Hawley, in *Advances in X-ray Analysis,* edited by K. Heinrich *et al.* (Plenum, New York, 1972), Vol. 15, p. 516.
[9]Crystal Products Bulletin, Union Carbide Corp., Czochralski Spinel.
[10]T. C. Damen, S. P. S. Porto, and B. Tell, Phys. Rev. **142,** 570 (1966).
[11]It should be noted that, in fact, the extent of nonstoichiometry is not known for the specific natural crystal studied here.
[12]S. Hafner and S. Laves, Z. Kristallogr. **115,** 321 (1961).
[13]E. Brun and S. Hafner, Z. Kristallogr. **117,** 37 (1962).
[14]R. W. G. Wyckoff, *Crystal Structure* (Interscience, New York, 1965), Vol. 3, p. 77.